Energetic negative ion source for fusion at NIFS (invited)

doi: 10.1063/1.1146854

Energetic negative ion source for fusion at NIFS (invited)

T. Kuroda, O. Kaneko, Y. Takeiri, Y. Oka, K. Tsumori, E. Asano, T. Kawamoto, and R. Akiyama
National Institute for Fusion Science, Nagoya 464-01, Japan

A. Ando
Department of Electrical Engineering, Faculty of Engineering, Tohoku University, Aoba, Sendai, 980-77, Japan

T. Takanashi and M. Hamabe
The Graduate University for Advanced Studies, Oroshi-cho, Toki-shi, Gifu, 509-02, Japan

(Presented on 13 September 1995)

Large high current hydrogen negative ion sources have been developed for the negative ion based neutral beam injector of the Large Helical Device (LHD) at NIFS. The prototype of the negative ion source is required to deliver a negative ion beam of 45 A at the beam energy of 125 keV. The optimization of 1/3 scale ion sources which are multicusp ion source with a rod and an external magnetic filter, respectively, has been investigated for the operation parameter of the plasma source. A total H^- current of 16 A is extracted at an operating pressure of 0.9–0.45 Pa with Cs seeding operation. Negative hydrogen ion current is proportional to the input arc power and a beam current density of 45 mA/cm^2 is attained. The beam extraction and acceleration characteristics are studied for a single-stage and a two-stage acceleration electrode. A beam divergence angle of 5 mrad is obtained. The results of research and development of a hydrogen negative ion source at NIFS will be reviewed. © *1996 American Institute of Physics.* [S0034-6748(96)04602-9]

I. INTRODUCTION

Neutral beam injection heating has become the most promising and reliable heating method. In advanced future tokamaks like ITER, a negative ion based neutral beam injector is required because negative ion beams have a much more effective neutralization efficiency at energy higher than 100 keV. High current negative ion source development has been intensively pursued for neutral beam injection and negative ion sources have progressed in performance.

On the Large Helical Device (LHD)[1] which is the main project of National Institute for Fusion Science and is the world's biggest superconducting heliotron/torsatron, a hydrogen neutral beam with a power of 20 MW at the beam energy of 125 keV has been planned to heat the target plasma up to 10 keV and a negative ion based NBI system is adopted. Here a high current negative ion source which delivers a negative ion beam of 45 A with a current density of 30 mA/cm^2 is required in the NBI design. A multicusp ion source with a magnetic filter has been investigated to meet the requirements of the negative ions. This article describes the results of research and development of high current hydrogen negative ion source at NIFS.

II. OPTIMIZATION OF NEGATIVE ION SOURCE

A. 1/3 scale negative ion source

According to results from high current negative ion sources during the last decade, there is a design principle for volume production negative ion sources, which is known as the tandem negative ion source concept.[2–4] In addition, it has been demonstrated that a Cesium seeding operation of a volume production source enhances the yield of negative ion current.[5] After experiments into fundamental properties for the optimization of the 1/6 scale negative ion source with small ion current, intense energetic negative ion source experiments have been carried out in a 1/3 scale negative ion source for NBI on LHD.

The schematic diagram of the 1/3 scale negative ion source is shown in Fig. 1(a). The plasma chamber is a multicusp-type source and the size of the chamber is 37 cm in width, 62.5 cm height, and 18.5 cm in depth. A short depth chamber is adopted. The plasma source is divided into a driver region and a beam extraction region by a water-cooled rod-type magnetic filter. A thin molybdenum liner is attached to the inner wall to avoid Cs condensation. The plasma source is designed to optimize the number of filament for plasma uniformity and discharge stability to produce sufficient density and depth of the chamber for power efficiency. Up to 48 filaments can be installed as the cathode in the arc chamber, but usually a lesser number of filament is used for discharges of up to 2000 A at a discharge voltage 150 V. Hairpin tungsten filament of 1.5 mm in diameter is usually used in the experiment. A small box structure surrounding each extraction hole, which is called an Egg Box Cell, is placed on the plasma grid.[6]

The accelerator is composed of four grids: a plasma grid, an extracting grid, an electron suppressing grid, and a ground grid. Each of the grids has 560 extraction holes of 9 mm in diameter in an area of 25×44 cm^2. The plasma grid is made of molybdenum without water cooling to keep it at high temperature during Cs operation. The others are made of

 0034-6748/96/67(3)/1114/6/$10.00

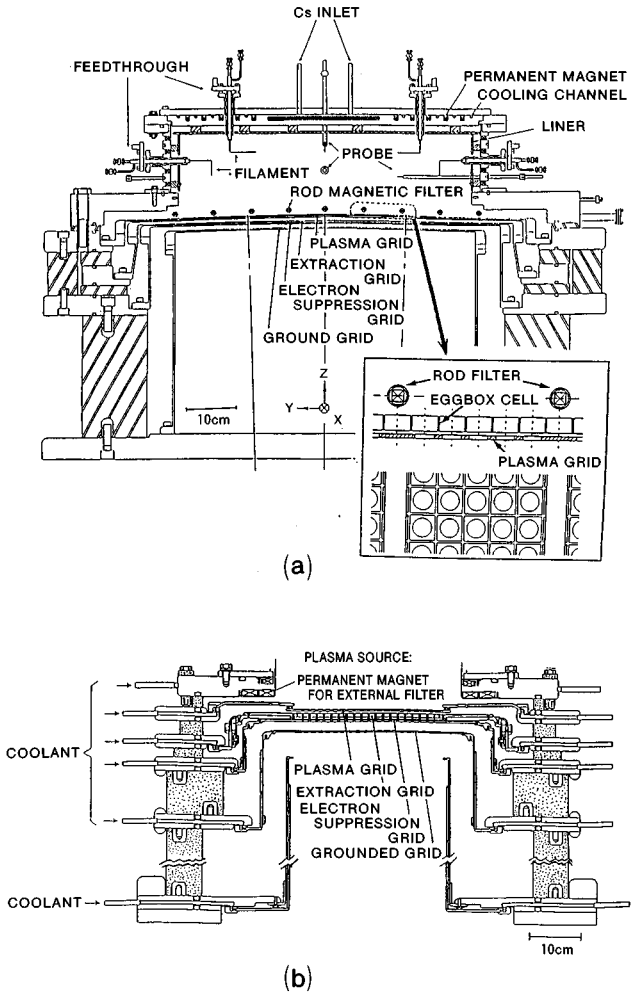

FIG. 1. A schematic drawing of the 1/3 scaled multicusp negative hydrogen negative ion source, (a) a rod-type source and (b) a external filter-type source.

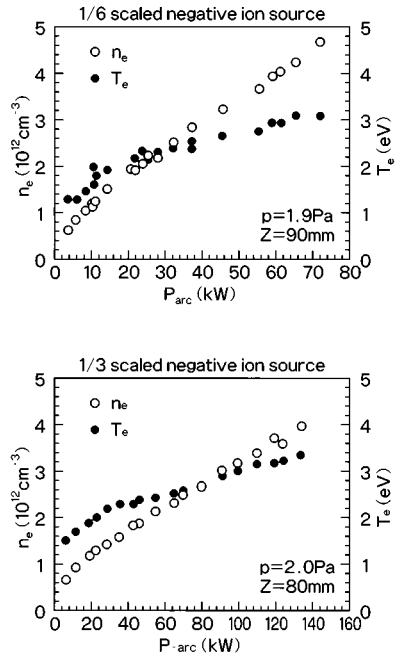

FIG. 2. The electron density and the electron temperature of the drive region as a function of the arc power for 1/6 and 1/3 scaled source.

oxygen-free copper and are partially water cooled. Each grid is divided into two subgrids, both of which face towards the focal point 6 m downstream from the ion source. The extracting grid of 10 mm in thickness has electron-bending magnets to eliminate electrons extracted with negative ions and cooling channels.

Although several types of magnetic filters have been tested,[7] we have examined the source performance for the rod filter and the external magnetic filter. In the former case, a filter magnetic field is produced by several rods of 1 cm diameter having the sector magnets inside. The line-integrated strength of the filter field is about 250 G cm. The gap between the rods and the plasma grid is typically about 1 cm.

The external magnetic filter is provided by a pair of permanent magnetic arrays embedded facing each other on the discharge chamber walls. The permanent array is 745 mm in length, 10 mm in thickness, and 60 mm in width (magnetization direction). The strength of the filter field is distributed over a large region and is about 70 G in the center. The line-integrated filter field strength is about 850 G cm. The dimension of the plasma source is nearly equal to that of the rod filter ion source. The extraction electrode system consists of five grids including an acceleration grid, but each of the grids has 522 extraction holes of 11.3 mm in diameter in an area of 25×50 cm^2. The Egg Box cell and the thin molde-num liner (as in the rod filter source) are not used.

Cesium is seeded into the discharge chamber through valves from Cs ovens. The amount of Cs is varied by the oven temperature and the opening duration of the valve. A small amount of Cs vapor is seeded once before starting operation, and no more Cs is supplied afterward. Both of the sources are operated with the pulse length of 0.3 s.

The H^- ion current is measured by using a two-dimensional calorimeter array which has a cross shape by which both horizontal and vertical beam profile can be measured in a shot. Also, two calorimeters are located at each of two points about 2.3 and 5 m downstream from the plasma grid.

B. Plasma source performance

Figure 2 shows the electron density and the electron temperature of the driver region as a function of the arc power for the 1/3 and 1/6 scale sources under nearly the same operating condition without Cs. Almost the same plasma parameters are obtained for the same arc power density. The larger the arc chamber is, the higher the required power. When the plasma confinement of the source is improved by reducing the plasma loss region near the rod filter flange, the electron density and temperature increase nearly twice for the same input power. An example of the density profile of the plasma is shown in Fig. 3 for the 1/3 scale source. In the operation with Cs, the discharge voltage becomes lower with increasing the amount of Cs.

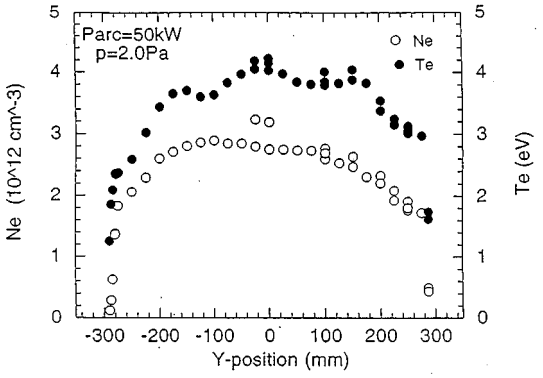

FIG. 3. An example of density profile of plasma.

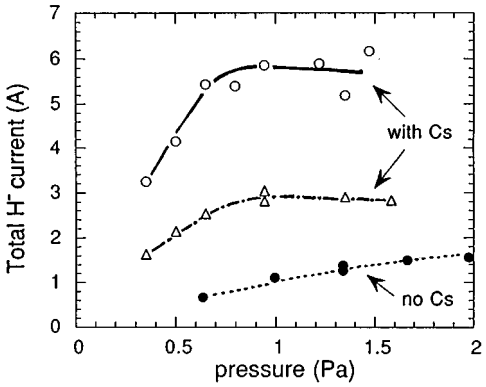

FIG. 5. Total H^- ion current as a function of the operating gas pressure of the plasma source.

C. Negative ion extraction characteristics

Important engineering and physical issues for the high performance negative ion source are achievement of (1) higher current density of hydrogen negative ion at low-pressure plasma source operation, (2) lower fraction of extracted electron current to negative ion current, and (3) low divergence of the ion beam. The dependencies of total H^- ion current on the plasma source operation parameters are examined by optimization of bias and temperature of the plasma grid in some cases. Figure 4 shows the dependence of the H^- ion current on the input arc power for the rod filter type and the external filter type, respectively. The H^- current increases nearly with the arc power in the case of operation with Cs. The H^- current of around 16 A is attained in the both ion sources but the arc efficiency is higher in the external filter type source than in the rod filter type source. The corresponding current density for the rod filter source is 45 mA/cm^2, in which the temperature of the grid rises to about 300 °C during operation. A grid temperature of 300 °C is consistent with the results on 1/6 scaled source.[6] The H^- ion current is enhanced three times by the Cs seeding operation. Simultaneously, the electron extraction current and the operating gas pressure are reduced by Cs seeding. Total H^- ion current is shown as a function of the gas pressure in Fig. 5 for different arc power in both sources. Total H^- current increases with increasing operation pressure in Cs operation and is saturated at a gas pressure of about 1 Pa or gradually decreases. The optimum operating gas pressure for the H^- ion current increases gradually as the arc power increases. The decrease of H^- current seems to be due to the increase of the stripping loss of the extraction electrode.

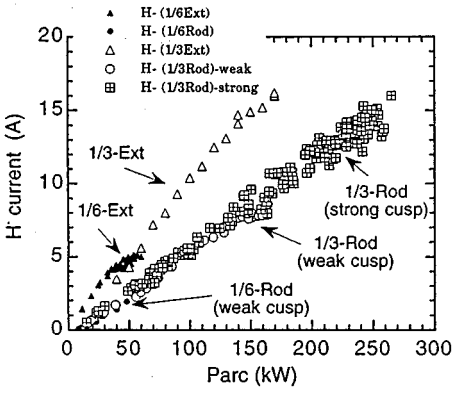

FIG. 4. Total H^- ion current as a function of the arc power of the plasma source.

Reduction of the ratio electron extracted current to negative hydrogen current and enhancement of negative ion production can be realized by biasing the plasma grid.[6] The H^- current reaches a maximum when biasing the plasma grid near the plasma potential and the extraction current which includes the extracted electron current decreases with the increase of the bias voltage to a level which is positive with respect to the plasma potential.

III. BEAM EXTRACTION AND ACCELERATION CHARACTERISTICS

Beam extraction and acceleration studies have been carried out into the fundamental properties of the 1/3 scale rod filter source with a single-hole electrode of 9 mm in diameter and into the large current properties of the 1/3 scale external filter source with a multihole electrode system, respectively. Single- and two-stage acceleration have been examined for both sources. In single-stage acceleration,[7] a three electrode system—plasma grid, extraction grid, and ground grid—is used for both sources.

Figure 6 shows the H^- current and the extraction current as a function of the extraction voltage for extraction grid gap lengths of 3 and 5 mm. The H^- current increases according to the space charge limited characteristic, Child–Langmuir law as mentioned elsewhere.[6] The square ratio of the effective extraction gap length is 1.57, which is a little larger than the extraction current ratio for extraction grid length of 5 and 3 mm. Figure 7 shows H^- ion current as a function of beam energy in two-stage acceleration. The envelope of optimum H^- ion current indicates the 3/2 power dependency on the beam energy. Since the H^- ion currents are extracted according to the Child–Langmuir law,[6] this indicates that the acceleration field affects the H^- ion extraction. A H^- ion current of 13.6 A is accelerated to 125 keV.

Figure 8(a) shows the dependence of the divergence angle on the acceleration voltage V_{acc}. Each curve corresponds to different current densities and an adequate V_{ext} is

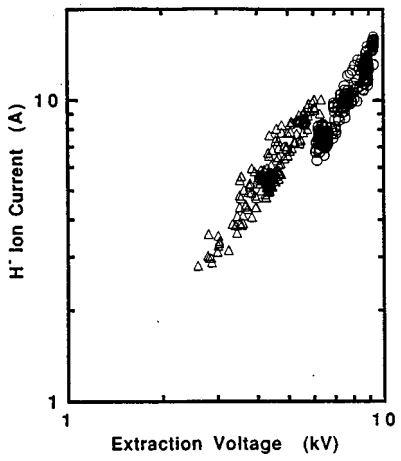

FIG. 6. The H^- current as a function of extraction voltage (external filter source).

applied in order that the H^- current saturation due to space charge does not occur. The optimum divergence angle of 5 mrad is obtained at each current density by adjusting V_{acc}. There is no effect on I_{acc} when V_{acc} changes as shown in Fig. 8(b). This indicates that I_{acc} is independent of the electric field in the acceleration gap and also of the beam trajectory in the gap.

Figure 9 shows the dependence of the beam divergence angle on the ratio of the acceleration electric field E_{acc} to the extraction electric field E_{ext}. The optimum ratio for the minimum divergence is 1.6 and is almost same value at different arc powers.

In the multibeam acceleration, the 1/2 half width is shown as a function of the acceleration voltage in Fig. 10. The divergence angle also changes by changing the acceleration voltage with a behavior similar to the single-hole case. In two-stage acceleration, the beam divergence is shown as a function of E_{acc}/E_{ext} for the multihole case in Fig. 11. The beam divergence can be optimized by changing the ratio of the first-stage voltage to the extraction voltage at the constant ratio of the first to the second acceleration electric field. From the results of the single-hole experiment, we find that there is a optimum value of E_{acc}/E_{ext} at about 1.5, which is almost as same as the optimum ratio of V_{acc}/V_{ext} in the single-stage acceleration. The optimum value of the ratio is not changed when the current density changes from 15 to 30 mA/cm^2. The beam divergence of the single beamlet is optimized to within 5 mrad and the beam divergence of the multibeamlet to within 10 mrad. The beam divergence is much more sensitive to E_{acc}/E_{ext} in the single-stage acceleration than it is in the two-stage acceleration.

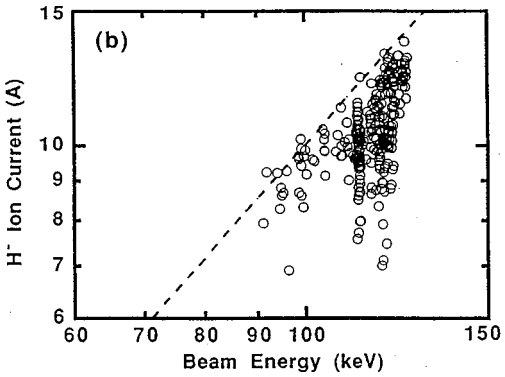

FIG. 7. The H^- current as a function of beam energy. The gas pressure is 0.45 Pa (external filter source).

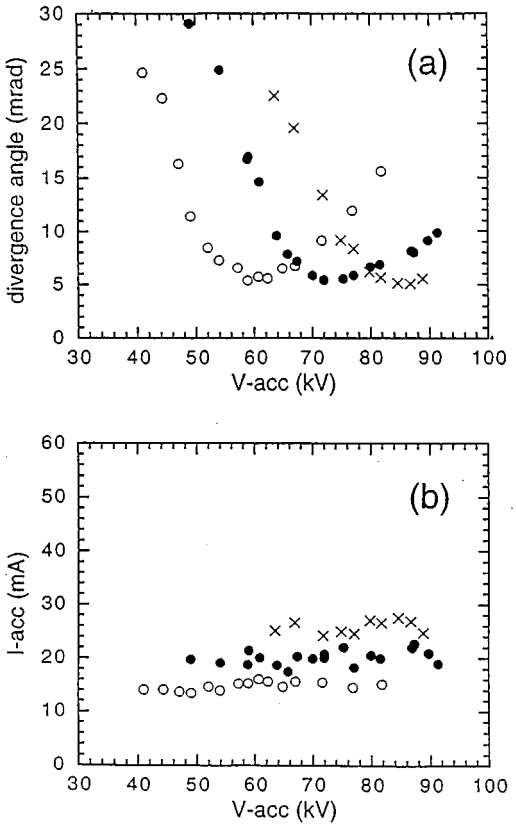

FIG. 8. Dependence of (a) the beam divergence angle and (b) I_{acc} on V_{acc} at $p=0.7$ Pa for three different H^- current density in the single-stage acceleration, with a single hole of 9 mm in diameter. (open circle) $P_{arc}=251$ W, $V_{ext}=6.3$ kV, $j=15$ mA/cm^2; (closed circle) $P_{arc}=35$ kW, $V_{ext}=7.9$ kV, $j=22$ mA/cm^2; (cross) $P_{arc}=45$ kW, $V_{ext}=9.3$ kV, $j=28$ mA/cm^2.

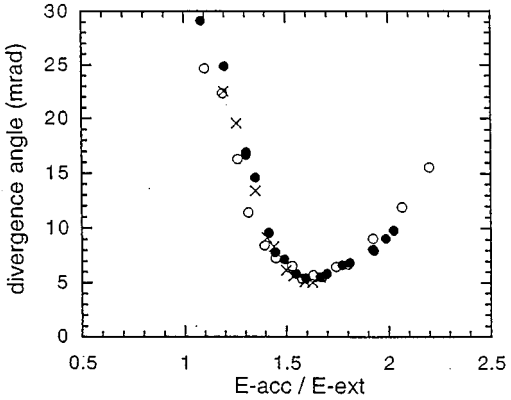

FIG. 9. Dependence of the beam divergence angle on E_{acc}/E_{ext} (single hole). (open circle) $P_{arc}=251$ W, $V_{ext}=6.3$ kV, $j=15$ mA/cm^2; (closed circle) $P_{arc}=35$ kW, $V_{ext}=7.9$ kV, $j=22$ mA/cm^2; (cross) $P_{arc}=45$ kW, $V_{ext}=9.3$ kV, $j=28$ mA/cm^2.

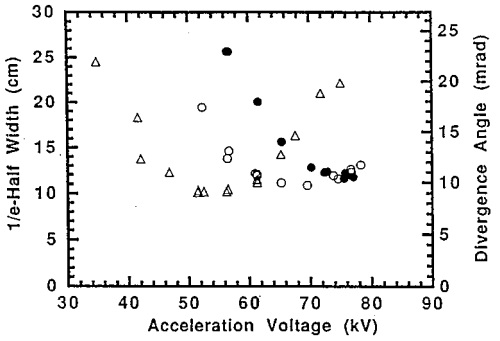

FIG. 10. e-folding half width of the vertical profile 11.2 m downstream in the single-stage acceleration as a function of the acceleration voltages of 5.2 (○), 4.3 (●), and 3.4 (△) keV. The gross divergence angle corresponding to the e-folding half width is also indicated on the right-hand axis. The arc power is 60 kW.

Figure 12 shows (a) the FWHM of the horizontal profile, and (b) the H^- ion current and the ratio of the second acceleration current to the H^- ion current as a function of the ratio of the second to the first acceleration electric field at the constant ratio of the first acceleration to the extraction. The profile, H^- ion current, and the current ratio are not changed significantly by changing the electric field ratio E_{acc2}/E_{acc1}. The optimum E_{acc1}/E_{ext} is higher in the longer extraction gap than in the short extraction gap. However, the optimum E_{acc2}/E_{acc1} is still 1.0–1.1 at the E_{acc1}/E_{ext} of about 1.4 or more.

In the multibeam extraction experiment in the external filter source, the acceleration electrode system in which the apertures of the grounded grid are displaced to steer all 270 beamlets to a focal point, is used for the optimization experiment of the beam acceleration. The multibeamlets are successfully focused and although the negative ion beamlets are deflected line by line to the opposite direction by the magnetic field for the electron deflection on the extraction grid, this steering is well compensated. As a result the gross divergence angle is 9 mrad.

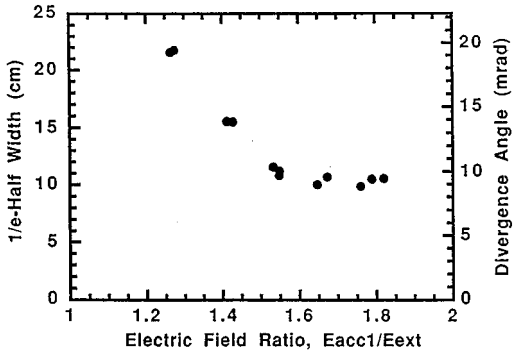

FIG. 11. e-folding half width of the vertical profile measured 11.2 m downstream from the ion source as a function of the ratio of the first acceleration to the extraction electric fields, E_{acc1}/E_{ext}, in the two-stage acceleration.

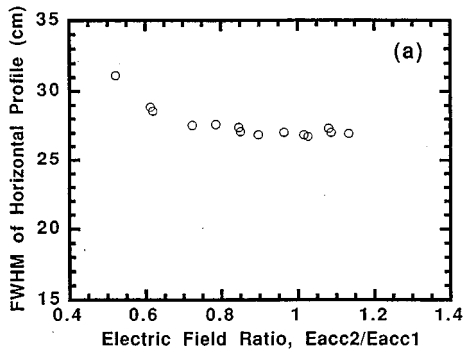

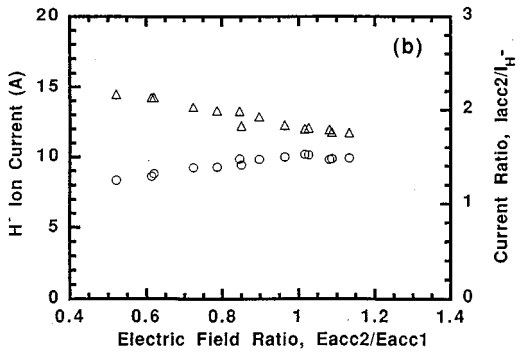

FIG. 12. (a) FWHM of the horizontal profile, and (b) the H^- ion current (open circles) and the ratio of the second acceleration current to the H^- ion current, I_{acc2}/I_{H^-} (open triangles) as a function of the ratio of the second to the first acceleration electric fields, E_{acc2}/E_{acc1}. The ratio of the first acceleration to the extraction electric field is a constant 0.98. The extraction gap length is 3 mm. The arc power is 90 kW and the gas pressure is 0.45 Pa.

IV. SUMMARY

In order to achieve a high current negative ion source of NBI on LHD, the 1/3 scale negative ion sources with a rod filter and a external filter have been investigated in order to optimize the plasma source parameter, the extraction, and the acceleration with Cs operation. About 16 A of the negative ion current is extracted at the operating gas pressure of 0.45 Pa and the corresponding current density is much higher than 45 mA/cm^2. A 13.6 A H^- ion beam has been accelerated to 125 keV at an operating gas pressure of 0.45 Pa with two-stage acceleration in the external filter type source. The arc efficiency of 0.1 A/kW is obtained with 16.2 A of the H^- ion current with an energy of 47 keV. The arc efficiency is higher in the external filter than in the rod filter. This higher arc efficiency of the external filter source is due to the reduction of the disadvantageous masking of the rod filter by the plasma grid which can lead to the loss of the plasma near the plasma grid into the rod. However, it is not clear that the effectiveness is due to the external filter only since the confinement cusp magnetic field and the magnetic field for the electron suppression are also strengthened.

Optimization of negative ion sources using the plasma source parameters tells us that (1) the negative ion current is proportional to the arc power which determines the plasma density and then the plasma source dimension and the required arc power can be decided by using an empirical scal-

ing law, (2) the H^- current density is optimized varying the operating gas pressure at constant arc power and the optimum gas pressure shifts to higher pressure with increasing arc power. The improvement of plasma confinement is an important issue for the ion source operation at the high beam current density with lower operating gas pressure.

The extraction characteristics according to the Child–Langmuir law are observed in the intense negative current extraction with the multiaperture source but the perveance is less than that of hydrogen negative ion.

In both the single-stage and two-stage acceleration, variation of beam divergence is qualitatively similar and minimum beam divergences of 5 and 9 mrad are obtained by adjusting the ratio of the acceleration electric field to the extraction electric field, E_{acc1}/E_{ext} for the single-hole and the multihole source.

Beam divergence is less sensitive for the two-stage acceleration than for the single-stage acceleration. The single-stage acceleration is useful to obtain an intense negative ion beam with a sufficiently small divergence as required by the NBI of LHD at the beam energy of 125 keV.

It is concluded that the aperture displacement technique is useful for focusing an intense negative ion beam by steering.

[1] A. Iiyoshi, Proceedings of the 13th Symposium on Fusion Engineering, Knoxville (1989), p. 1007.
[2] M. Bacal *et al.*, Rev. Sci. Instrum. **50**, 719 (1979).
[3] M. Bacal and G. W. Hamilton, Phys. Rev. Lett. **42**, 1538 (1979).
[4] K. N. Leung *et al.*, Rev. Sci. Instrum. **54**, 56 (1983).
[5] Y. Okumura *et al.*, Proc. of the 16th Symposium on Fusion Technology (1990), p. 1026.
[6] A. Ando *et al.*, *6th International Symp. on Production and Neutralization of Negative Ions and Beams*, 1992, Brookhaven (AIP, New York, 1992), AIP Conf. Proc. No. 287, p. 339.
[7] M. Hanada *et al.*, Rev. Sci. Instrum. **61**, 499 (1990).